Narrow Optical Homogeneous Linewidths in Rare Earth Doped Nanocrystals

A. Perrot,[1] Ph. Goldner,[1] D. Giaume,[1] M. Lovrić,[1] C. Andriamiadamanana,[1] R. R. Gonçalves,[1,2] and A. Ferrier[1,*]

[1]*Chimie ParisTech, Laboratoire de Chimie de la Matière Condensée de Paris, CNRS-UMR 7574, UPMC Université Paris 06, 11 rue Pierre et Marie Curie 75005 Paris, France*

[2]*Departamento de Química, Faculdade de Filosofia, Ciências e Letras de Ribeirão Preto, Universidade de São Paulo, Avenida Bandeirantes, 3900, CEP 14040-901, Ribeirão Preto, SP, Brazil*

(Received 13 July 2013; published 12 November 2013)

A homogeneous linewidth of 85.6 ± 4.4 kHz is reported in 60 nm Eu^{3+} doped Y_2O_3 nanocrystals at 1.3 K. This linewidth was measured by two-pulse photon echoes on highly scattering powders using heterodyne detection. Spectral diffusion was also investigated by three-pulse photon echoes and resulted in a limited broadening of the homogenous linewidth of about 250 kHz over 120 μs. Compared to achievable Rabi frequencies, in the range of several MHz, these values show that rare earth doped nanocrystals can be useful for applications in optical quantum information processing.

DOI: 10.1103/PhysRevLett.111.203601 PACS numbers: 42.50.Md, 42.70.−a, 76.30.Kg, 78.67.Bf

Nanostructured optical materials have potential applications in nanoscale sensing, imaging, and quantum information processing (QIP). Long spin coherence and efficient optical readout of defect centers in nanodiamonds have been used to demonstrate hybrid quantum systems [1], highly sensitive magnetic field detectors [2], or imaging [3]. QIP could be performed with quantum dots strongly coupled to a nanocavity [4] or with single defects in nanostructured silicon [5,6]. Providing extremely narrow optical and nuclear spin transitions [7,8], rare earth (RE) ion doped crystals are especially promising for optical QIP. Indeed, photonic quantum storage [9–11], quantum gates [12], and qubit arbitrary rotations [13] have been demonstrated in these materials. However, these experiments were performed in bulk crystals, which prevents further advances, like coupling to nanocavities [14] or other nanoscale quantum systems [1], and efficient single rare earth detection. The latter, a key element in quantum technologies [15,16], has been recently achieved in nanostructured silicon [6] and nanoparticles [17]. However, the interest of nanostructuration is largely determined by the coherence lifetimes which can be achieved, as dephasing in nanoscale materials can be much stronger than in bulk crystals [2]. In particular, previous studies on RE doped nanocrystals [18–22] reported homogeneous linewidths between 5 and 50 MHz, whereas typical Rabi frequencies which can be obtained for RE transitions are in the MHz range [23]. These transitions were therefore too broad to be used in QIP.

Here, we report a homogeneous linewidth of 85.6 ± 4.4 kHz (coherence lifetime $T_2 = 3.7 \pm 0.2$ μs) in 60 nm nanocrystals of europium doped Y_2O_3 at 1.3 K. To our best knowledge, it is the narrowest optical transition reported for any nanocrystal. It was measured on powders using our recent observation of photon echoes in highly scattering media [24]. Especially, we took advantage of the surprisingly high spatial correlation between echo and excitation fields to implement a sensitive heterodyne detection scheme. Three-pulse photon echoes also revealed limited spectral diffusion over longer times, allowing repeated optical addressing of ions on a 100 μs time scale after spectral selection. Our results show that RE doped nanocrystals could be useful in quantum processing applications.

Experiments were performed on 0.86 at. % Eu^{3+} : Y_2O_3 nanocrystals obtained by a solvothermal method [25]. X-ray diffraction showed that the phase of the crystals is cubic (space group Ia3), like that of bulk single crystals. Using x-ray diffraction and transmission electron microscopy, we found a crystallite size of 60 ± 5 nm. The value was similar for different crystalline orientations, which indicates an isotropic growth.

Figure 1(a) shows the experimental arrangement for photon echo experiments. The output of a 1 MHz linewidth dye laser (Coherent 899-21) was focused on the nanocrystals in the form of a powder, which filled a hole in a copper plate of 2 mm diameter and 0.5 mm thickness. Two glass windows maintained the powder on each side of the copper plate to enable transmission experiments. The assembly was placed in a helium bath cryostat. The laser frequency was set to 580.88 nm (vacuum) in resonance with the Eu^{3+} $^5D_0$-$^7F_0$ transition. The powder caused strong scattering of the transmitted light and a speckle pattern [Fig. 1(b)], limited by the cryostat windows apertures, formed up. Ballistic transmission was less than 5×10^{-6}. The scattered light transmitted through the powder was collected by a 75 mm diameter lens and focused on a 50 MHz bandwidth avalanche photodiode (Thorlabs APD 110A). An acousto-optic modulator, operating in a double pass configuration, provided pulse shaping and frequency shifting of the excitation light. To avoid bleaching of the transition by spectral hole burning, the laser was continuously scanned over 1 GHz within 1 s. Incident laser power was up to 80 mW. To enhance detection, we took

 © 2013 American Physical Society

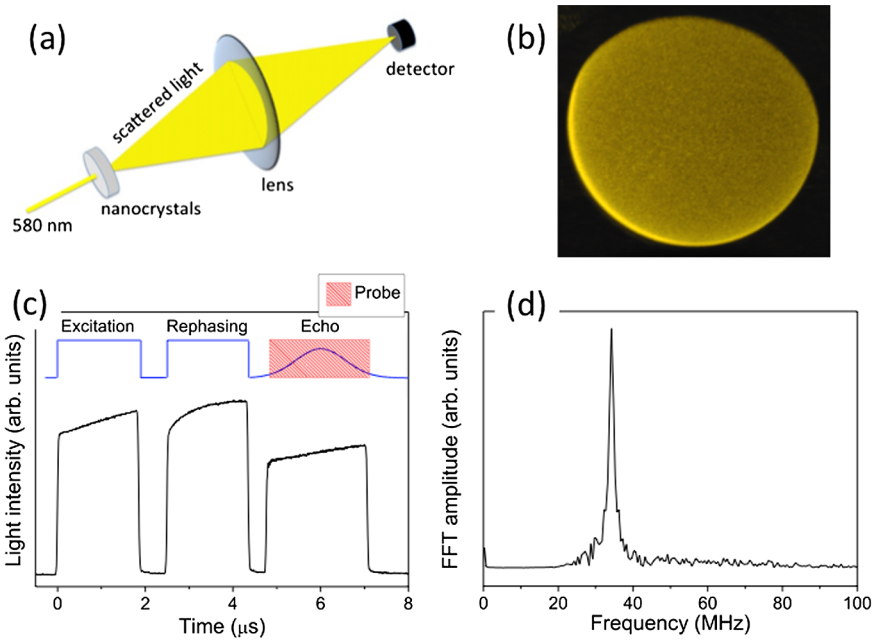

FIG. 1 (color online). Photon echo experiments on powders of nanocrystals. (a) Experimental scheme. (b) Speckle pattern observed for transmitted light through the powder. (c) Schematic two-pulse photon echo sequence (top, echo pulse not to scale) and corresponding signal (bottom). The probe pulse is shifted by 34 MHz for heterodyne detection. (d) Averaged fast Fourier transform (FFT) of the heterodyne detection beat signal after a 20 MHz cutoff high pass filter.

advantage of the high spatial correlation between the speckles produced by the echo and the laser, which enabled heterodyne detection [24]. A typical two-pulse photon echo sequence and the corresponding signal are shown in Fig. 1(c). The first pulse excites the atoms coherences and shows an intensity variation corresponding to a strongly damped nutation [26]. This is attributed to two effects: (i) the simultaneous excitation of optical transitions, between ground and excited state hyperfine levels, with different strengths [27] and (ii) the spread in Rabi frequencies due to light scattering in the powder. The second pulse reverses the phase evolution of the atoms. At this time, the atoms have already acquired a significant dephasing and the shape of the second pulse corresponds to an incoherent population transfer. The echo appears at $t = 6\ \mu$s and beats with the probe pulse, which is shifted in frequency by 34 MHz compared to the two first pulses. This frequency was chosen for the best signal-to-noise ratio (SNR). Averaging the Fourier transform of the detected heterodyne pulse amplitude for 200 times results in a photon echo signal with SNR = 15; see Fig. 1(d).

The low temperature absorption spectrum of the Eu^{3+} $^5D_0$-$^7F_0$ transition is shown in Fig. 2. The absorption line is well described by a Lorentzian profile with a full width at half maximum (FWHM) of 17 GHz. This value is remarkably close to the widths reported for single crystals [28], showing that our nanocrystals have a high crystalline quality. This is confirmed by the Lorentzian shape of the absorption spectrum, which corresponds to strains caused by Eu^{3+} ions themselves [29]. From the absorption coefficient of a bulk crystal, we deduced an average light propagation length of 2.8 mm in the 0.5 mm thick powder, which is consistent with the relatively strong echo signals observed.

Homogeneous linewidths at different temperatures were determined from decays of the photon echo amplitude as a function of pulse separation [30] and are shown in Fig. 3. The decays were found to be close to an exponential [Fig. 4 (circles)]. At 1.3 K, the transition coherence lifetime was $3.7 \pm 0.2\ \mu$s corresponding to a homogeneous linewidth Γ_h of 85.6 ± 4.4 kHz. This is 1–2 orders of magnitude narrower than previously reported values in rare earth doped nanocrystals like Eu^{3+}: Y_2O_3 (monoclinic phase)

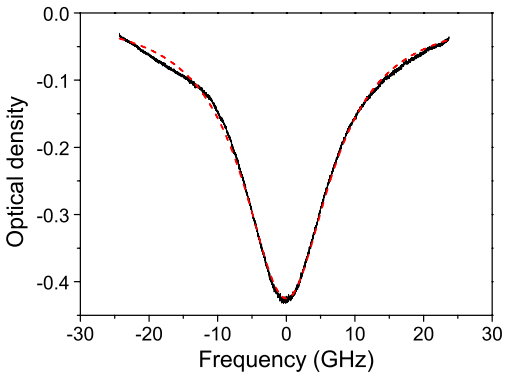

FIG. 2 (color online). Absorption spectrum of 0.86 at. % Eu^{3+} : Y_2O_3 nanocrystals at 3.5 K (black solid line) and Lorentzian fit (red dashed line).

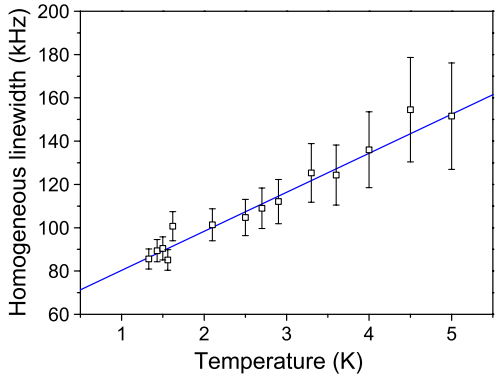

FIG. 3 (color online). Temperature dependence of the homogeneous linewidth Γ_h measured by two-pulse photon echoes. The solid line represents the linear fit to $\Gamma_h = \Gamma_0 + RT$ with $\Gamma_0 = 62 \pm 3$ kHz and $R = 18 \pm 1.6$ kHz/K.

[18] or $Pr^{3+}:LaF_3$ (embedded in a glass matrix) [22]. Possible explanations for this difference are the large size of our nanocrystals, which could reduce surface related dephasing, and their high crystalline quality, as evidenced by a Eu^{3+} narrow inhomogeneous linewidth (see above). Some previous studies also used spectral hole burning to determine Γ_h. This technique is only sensitive for long time scales and is inherently limited by the laser linewidth and thus generally not adapted to measuring narrow homogeneous linewidths. The Γ_h values reported in this Letter are also much lower than those observed in diamond nanocrystals or quantum dots, which are of the order of ≈ 1 GHz [31] and ≈ 100 MHz [32], respectively. In these two systems, however, Γ_h is limited by the excited state lifetime T_1, whereas in our nanocrystals, $T_1 = 970$ μs (similar to that of bulk crystals [33]), corresponding to a negligible contribution of 330 Hz to Γ_h. Narrow homogeneous linewidths result from the exceptional decoupling of rare earth ions from environment, which is due to the shielding of f electrons by closed shells. Our result demonstrates that this decoupling is effective, even in nanoscale materials. Indeed, in our nanocrystals, the homogeneous linewidths are comparable to those observed in $Eu^{3+}:Y_2O_3$ transparent ceramics with 50 μm single crystalline grains [34] and even to values reported in some bulk single crystals [33]. In these materials, dephasing mechanisms were attributed to fluctuations in magnetic field, due to impurities bearing a magnetic moment, and/or in strain due to two-level systems (TLSs). The latter were attributed to oxygen vacancies [33]. Coupling between the TLS and the rare earth results in an approximately linear temperature dependence of Γ_h [33,35], as observed in our nanocrystals (Fig. 3). Assuming for simplicity a linear dependence $\Gamma_h = \Gamma_0 + RT$, we found $\Gamma_0 = 62 \pm 3$ kHz and $R = 18 \pm 1.6$ kHz/K. As the slopes R determined in single crystals were in the range 1–10 kHz/K [33], it is likely that the nanocrystals also contain TLSs, possibly related to oxygen vacancies. Additional dephasing processes must, however, be present, since the homogeneous linewidth extrapolated at 0 K, where TLSs are frozen, is 62 kHz. In comparison, it can be as low as 760 Hz in the best $Eu^{3+}:Y_2O_3$ single crystals [36]. This difference could be due to impurities bearing a flipping magnetic moment, with a fast and temperature independent rate. The same dephasing process was suggested to explain the homogeneous linewidth of 59 kHz $Eu^{3+}:Y_2O_3$ in a transparent ceramic [34].

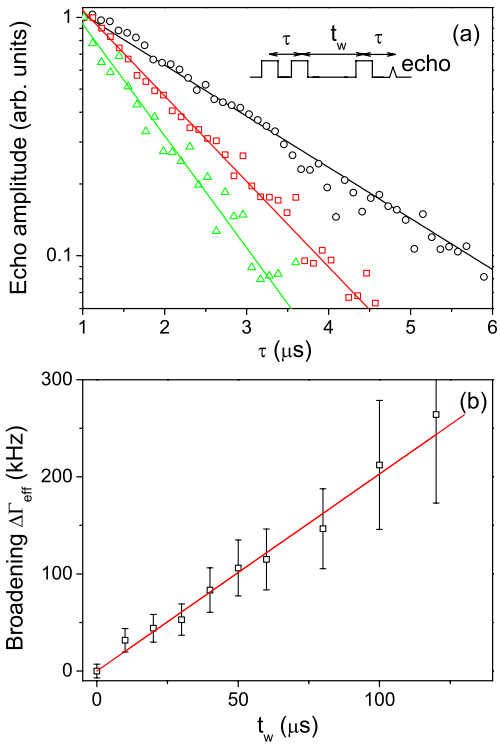

FIG. 4 (color online). (a) The circles represent the two-pulse photon echo amplitude decay as a function of pulse separation at 1.3 K. The squares (respectively, triangles) represent the three-pulse photon echo amplitude decays as a function of τ for $t_w = 10$ μs (respectively, 40 μs) at 2.7 K (inset: sequence scheme). Solid lines represent exponential fits. (b) Homogeneous broadening as a function of t_w. The solid line represents the linear fit with a 2 kHz/μs slope.

Spectral diffusion [30] is also a concern for repeated optical addressing of spectrally selected ions. It results in a time dependent broadening of the homogeneous linewidth and can be probed by three-pulse photon echoes, on time scales up to the excited state population lifetime T_1 [37]. In these experiments, the first two pulses, separated by a time τ, create a spectral grating by converting the initial coherence into ground and excited state populations. The third pulse, separated from the second one by a time t_w, is diffracted on this grating and produces an echo. Spectral diffusion, i.e., frequency shifts of the optical transition due to random fluctuations of the rare earth environment, gradually erases the grating during t_w, and the echo amplitude A is expressed as

$$A = A_0 \exp\left(-\frac{t_w}{T_1}\right) \exp[-2\tau\pi\Gamma_{\text{eff}}(\tau, t_w)], \quad (1)$$

where the effective linewidth Γ_{eff} depends on τ and t_w in the most general case. Echo amplitude decays were recorded at 2.7 K as a function of τ for t_w values between 0 and 120 μs. This range was limited by SNR since $T_1 =$ 970 μs. The decays were found to be exponential, indicating that Γ_{eff} depends only on t_w [Fig. 4(a)]. At $t_w = 0$, the three-pulse echo reduces to the two-pulse echo sequence and $\Gamma_{\text{eff}} = \Gamma_h$. Figure 4(b) shows that the homogeneous linewidth broadening $\Delta\Gamma(t_w) = \Gamma_{\text{eff}}(t_w) - \Gamma_h$ increases approximately linearly with increasing t_w, with a slope of 2 kHz/μs. Assuming a flipping rate of the impurities' magnetic moments larger than $1/T_2$, the corresponding dephasing results in a broadening effective on a time scale of τ and independent of t_w [37]. On the other hand, TLSs have broad flipping rate distributions affecting linewidths on very large time scales [38–40]. The homogeneous linewidth broadening over time $\Delta\Gamma(t_w)$ could therefore be attributed to the TLS identified in the previous section. Concerning quantum processing applications, the broadening of the homogeneous linewidth is $\Delta\Gamma \approx 250$ kHz over 120 μs, much smaller than the achievable Rabi frequencies (1–10 MHz). Once an ion or an ensemble of ions are spectrally selected, this would allow one to optically address them repeatedly over 120 μs. It would also be useful to measure $\Delta\Gamma$ over longer time scales by spectral hole burning. This was not possible with our setup since the laser had a frequency jitter of several MHz, which limited the width of the observed holes.

In conclusion, we have observed an 86 kHz homogeneous linewidth in 60 nm europium doped nanocrystals at 1.3 K. This was measured by photon echoes on a highly scattering powder, taking advantage of the high spatial correlation between exciting and echo fields to increase sensitivity by heterodyne detection. The observed homogeneous linewidth, about 2 orders of magnitude lower than achievable Rabi frequencies, and its limited broadening over time by spectral diffusion, 250 kHz on time scales of 120 μs, demonstrates the potential of rare earth nanocrystals in optical quantum information processing.

This work was supported by the European Union FP7 Projects QuRep (No. 247743) and CIPRIS (Marie Curie Action No. 287252) and the ANR Project RAMACO (No. 12-BS08-0015-01).

*alban-ferrier@chimie-paristech.fr

[1] O. Arcizet, V. Jacques, A. Siria, P. Poncharal, P. Vincent, and S. Seidelin, Nat. Phys. **7**, 879 (2011).
[2] G. Balasubramanian, I. Y. Chan, R. Kolesov, M. Al-Hmoud, J. Tisler, C. Shin, C. Kim, A. Wojcik, P. R. Hemmer, A. Krueger, T. Hanke, A. Leitenstorfer, R. Bratschitsch, F. Jelezko, and J. Wrachtrup, Nature (London) **455**, 648 (2008).
[3] P. Maletinsky, S. Hong, M. S. Grinolds, B. Hausmann, M. D. Lukin, R. L. Walsworth, M. Lončar, and A. Yacoby, Nat. Nanotechnol. **7**, 320 (2012).
[4] K. Hennessy, A. Badolato, M. Winger, D. Gerace, M. Atatüre, S. Gulde, S. Fält, E. L. Hu, and A. Imamoglu, Nature (London) **445**, 896 (2007).
[5] J. J. Pla, K. Y. Tan, J. P. Dehollain, W. H. Lim, J. J. L. Morton, F. A. Zwanenburg, D. N. Jamieson, A. S. Dzurak, and A. Morello, Nature (London) **496**, 334 (2013).
[6] C. Yin, M. Rancic, G. G. de Boo, N. Stavrias, J. C. McCallum, M. J. Sellars, and S. Rogge, Nature (London) **497**, 91 (2013).
[7] T. Böttger, C. W. Thiel, R. L. Cone, and Y. Sun, Phys. Rev. B **79**, 115104 (2009).
[8] E. Fraval, M. J. Sellars, and J. J. Longdell, Phys. Rev. Lett. **95**, 030506 (2005).
[9] C. Clausen, I. Usmani, F. Bussières, N. Sangouard, M. Afzelius, H. de Riedmatten, and N. Gisin, Nature (London) **469**, 508 (2011).
[10] E. Saglamyurek, N. Sinclair, J. Jin, J. A. Slater, D. Oblak, F. Bussières, M. George, R. Ricken, W. Sohler, and W. Tittel, Nature (London) **469**, 512 (2011).
[11] I. Usmani, C. Clausen, F. Bussières, N. Sangouard, M. Afzelius, and N. Gisin, Nat. Photonics **6**, 234 (2012).
[12] J. J. Longdell, M. J. Sellars, and N. B. Manson, Phys. Rev. Lett. **93**, 130503 (2004).
[13] L. Rippe, B. Julsgaard, A. Walther, Y. Ying, and S. Kröll, Phys. Rev. A **77**, 022307 (2008).
[14] D. L. McAuslan, J. J. Longdell, and M. J. Sellars, Phys. Rev. A **80**, 062307 (2009).
[15] J. H. Wesenberg, K. Mølmer, L. Rippe, and S. Kröll, Phys. Rev. A **75**, 012304 (2007).
[16] Y. Yan, J. Karlsson, L. Rippe, A. Walther, D. Serrano, D. Lindgren, M.-e. Pistol, S. Kröll, P. Goldner, L. Zheng, and J. Xu, Phys. Rev. B **87**, 184205 (2013).
[17] R. Kolesov, K. Xia, R. Reuter, R. Stöhr, A. Zappe, J. Meijer, P. R. Hemmer, and J. Wrachtrup, Nat. Commun. **3**, 1029 (2012).
[18] K. S. Hong, R. S. Meltzer, B. Bihari, D. K. Williams, and B. M. Tissue, J. Lumin. **76–77**, 234 (1998).
[19] R. S. Meltzer and K. S. Hong, Phys. Rev. B **61**, 3396 (2000).
[20] R. S. Meltzer, W. M. Yen, H. Zheng, S. P. Feofilov, M. J. Dejneka, B. M. Tissue, and H. B. Yuan, Phys. Rev. B **64**, 100201 (2001).
[21] R. M. Macfarlane and M. J. Dejneka, Opt. Lett. **26**, 429 (2001).
[22] R. S. Meltzer, H. Zheng, and M. J. Dejneka, J. Lumin. **107**, 166 (2004).
[23] For Eu^{3+}: Y_2SiO_5, a laser power of 1 mW focused to a spot of 1 μm diameter gives a Rabi frequency of 4.8 MHz.
[24] F. Beaudoux, A. Ferrier, O. Guillot-Noël, T. Chanelière, J.-L. Le Gouët, and P. Goldner, Opt. Express **19**, 15236 (2011).
[25] J. Yang, Z. Quan, D. Kong, X. Liu, and J. Lin, Cryst. Growth Des. **7**, 730 (2007).
[26] Y. Sun, G. M. Wang, R. L. Cone, R. W. Equall, and M. J. M. Leask, Phys. Rev. B **62**, 15443 (2000).
[27] B. Lauritzen, N. Timoney, N. Gisin, M. Afzelius, H. de Riedmatten, Y. Sun, R. M. Macfarlane, and R. L. Cone, Phys. Rev. B **85**, 115111 (2012).

[28] G. P. Flinn, K. W. Jang, J. Ganem, M. L. Jones, R. S. Meltzer, and R. M. Macfarlane, Phys. Rev. B **49**, 5821 (1994).
[29] F. Könz, Y. Sun, C. W. Thiel, R. L. Cone, R. W. Equall, R. L. Hutcheson, and R. M. Macfarlane, Phys. Rev. B **68**, 085109 (2003).
[30] R. M. Macfarlane, J. Lumin. **100**, 1 (2002).
[31] P. Siyushev, V. Jacques, I. Aharonovich, F. Kaiser, T. Müller, L. Lombez, M. Atatüre, S. Castelletto, S. Prawer, F. Jelezko, and J. Wrachtrup, New J. Phys. **11**, 113029 (2009).
[32] S. Ates, S. M. Ulrich, S. Reitzenstein, A. Löffler, A. Forchel, and P. Michler, Phys. Rev. Lett. **103**, 167402 (2009).
[33] G. P. Flinn, K. W. Jang, J. Ganem, M. L. Jones, R. S. Meltzer, and R. M. Macfarlane, J. Lumin. **58**, 374 (1994).
[34] A. Ferrier, C. W. Thiel, B. Tumino, M. O. Ramírez, L. E. Bausá, R. L. Cone, A. Ikesue, and P. Goldner, Phys. Rev. B **87**, 041102 (2013).
[35] R. M. Macfarlane, Y. Sun, R. L. Cone, C. W. Thiel, and R. W. Equall, J. Lumin. **107**, 310 (2004).
[36] R. M. Macfarlane and R. M. Shelby, Opt. Commun. **39**, 169 (1981).
[37] T. Böttger, C. W. Thiel, Y. Sun, and R. L. Cone, Phys. Rev. B **73**, 075101 (2006).
[38] H. C. Meijers and D. A. Wiersma, Phys. Rev. Lett. **68**, 381 (1992).
[39] H. Maier, B. M. Kharlamov, and D. Haarer, Phys. Rev. Lett. **76**, 2085 (1996).
[40] R. M. Macfarlane, Y. Sun, P. B. Sellin, and R. L. Cone, Phys. Rev. Lett. **96**, 033602 (2006).